



Елена Суровяткина

**ИСПОЛЬЗОВАНИЕ
БИФУРКАЦИОННОГО АНАЛИЗА
для распознавания и обнаружения
закономерностей сложной динамики
систем высокой размерности**

Институт космических исследований Российской академии наук

Содержание

Введение

Сложная, большая, multi-scale система

- ✓ **Описание модели и постановка задачи**
- ✓ **Бифуркационный анализ**
- ✓ **Инвариантное свойство
мультистабильности**
- ✓ **Приложения**

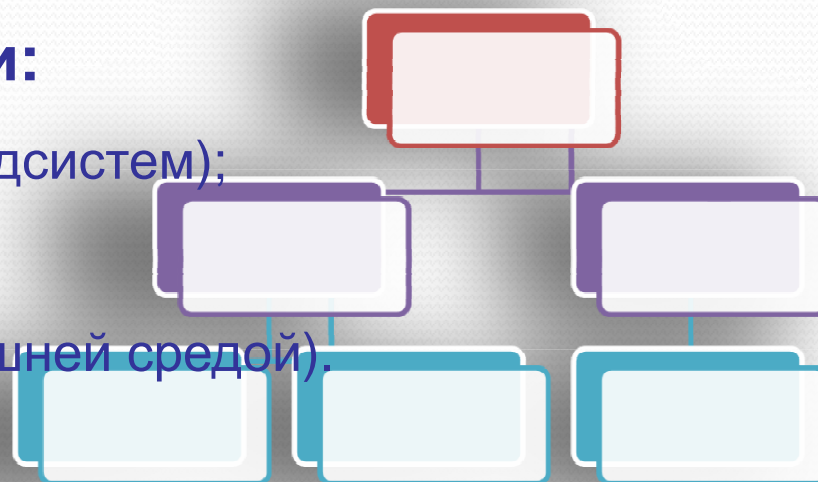
Заключение

БОЛЬШАЯ, MULTI-SCALE , LARGE-SCALE СИСТЕМА

“Большая система, управляемая система - совокупность взаимосвязанных управляемых подсистем, объединённых общей целью функционирования.”(БСЭ)

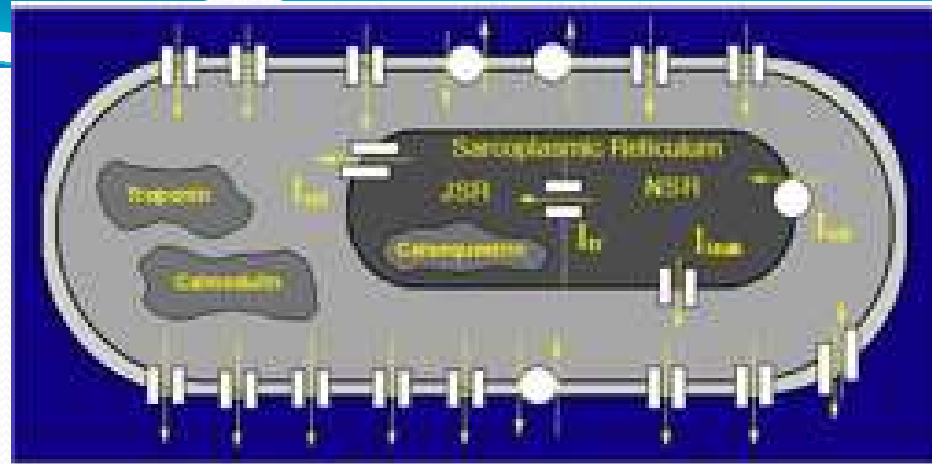
Характерные особенности:

- Наличие выделяемых частей (подсистем);
- Связи между подсистемами;
- Связь с другими системами (внешней средой).



Системный подход - исследование на раскрытие целостности объекта и обеспечивающих её механизмов, на выявление многообразных типов связей сложного объекта и сведение их в единую теоретическую картину.

Model



The rate of change of membrane potential is given by

$$dV/dt = (-I_{ion} + I_{stim}) / C$$

where

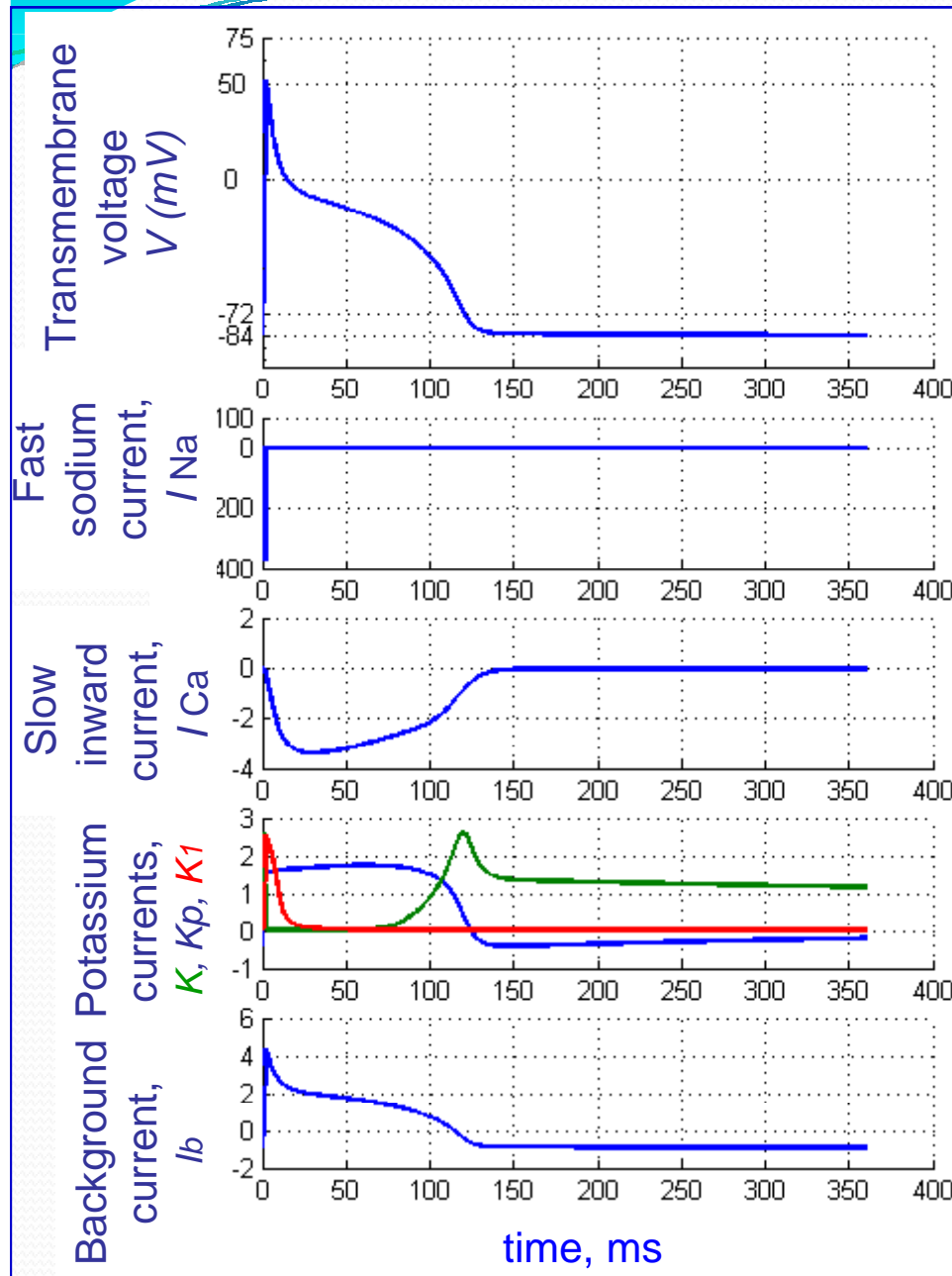
I_{ion} - the total ionic current density,

I_{stim} - a stimulus current,

C - the membrane capacitance

Luo-Rudy model

C. Luo and Y. Rudy. Circ. Res. Vol. 68
 No. 15, 1501-1526 (1991)



$$\frac{dV}{dt} = \frac{(-I_{ion} + I_{stim})}{C_m}$$

$$I_{ion} = I_{Na} + I_{Ca} + I_K + I_{K_1} + I_{Kp} + I_b$$

Ionic currents

$$I_{Na} = 23m^3h_j(V - E_{Na})$$

$$I_{Ca} = G_{Ca} \cdot d \cdot f \cdot (V - E_{Ca}),$$

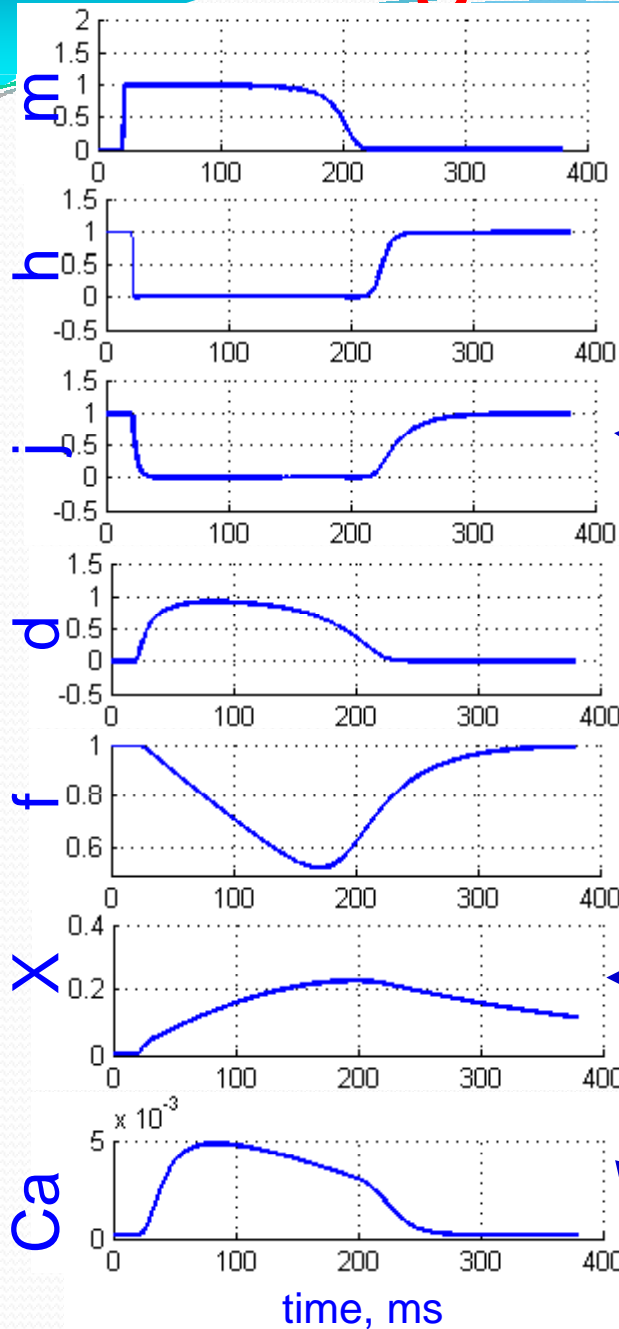
$$I_k = \bar{G}_k \cdot X \cdot X_i \cdot (V - E_k),$$

$$I_{k1} = \bar{G}_{k1} \cdot K1_{\infty} \cdot (V - E_{k1}),$$

$$I_{Kp} = 0.0183 \cdot K_p \cdot (V - E_{Kp}),$$

$$I_b = 0.03921 \cdot (V + 59.87)$$

Ionic gates



$$dy/dt = (y_{\infty} - y) / \tau_y$$

$$\tau_y = \frac{1}{\alpha_y + \beta_y} \quad y_{\infty} = \frac{a_y}{\alpha_y + \beta_y}$$

$$\alpha_y = f(V), \quad \beta_y = f(V)$$

$$I_{Na} = 23 m^3 h j (V - E_{Na})$$

$$I_{Ca} = G_{Ca} d f (V - E_{Ca}),$$

$$I_k = \bar{G}_k X X_i (V - E_k),$$

$$d([Ca]_i) / dt = -10^{-4} \cdot I_{Ca} + 0.07(10^{-4} - [Ca]_i)$$

$$dy/dt = (y_\infty - y) / \tau_y \quad y_\infty = \frac{\alpha_y}{\alpha_y + \beta_y} \quad \tau_y = \frac{1}{\alpha_y + \beta_y}$$

$$I_{Na} = 23m^3h_j(V - E_{Na})$$

For all range of V

$$\alpha_m = \frac{0.32(V + 47.13)}{1 - \exp[-0.1(V + 47.13)]}$$

$$\beta_m = 0.08 \exp\left(-\frac{V}{11}\right)$$

For $V > -40 \text{ mV}$

$$\alpha_h = a_j = 0$$

$$\beta_j = \frac{0.3 \exp(-2.535 \cdot 10^{-7} V)}{1 + \exp[-0.1(V + 32)]}$$

$$\beta_h = \frac{1}{0.13(1 + \exp[V + 10.66] / -11.1)}$$

For $V < -40 \text{ mV}$

$$\alpha_h = 0.135 \exp[(80 + V) / -6.8]$$

$$\beta_h = 3.56 \exp(0.079 V) + 3.1105 \exp(0.35 V)$$

$$\alpha_j = \frac{[-1.2714 \cdot 10^5 \cdot \exp(0.2444 V) - 3.474 \cdot 10^5 \cdot \exp(-0.04391 V)](V + 37.78)}{1 + \exp[0.311(V + 79.23)]}$$

$$\beta_j = \frac{0.1212 \cdot \exp(-0.01052 V)}{1 + \exp(-0.1378 (V + 40.14))}$$

$$I_{Ca} = G_{Ca} \cdot d \cdot f \cdot (V - E_{Ca}),$$

$$E_{Ca} = 7.7 - 13.0287 \cdot \ln([Ca]_i)$$

$$\alpha_d = \frac{0.095 \cdot \exp[-0.01(V - 5)]}{1 + \exp[-0.072(V - 5)]}$$

$$\beta_d = \frac{0.07 \cdot \exp[-0.017(V + 44)]}{1 + \exp[0.05(v + 44)]}$$

$$\alpha_f = \frac{0.012 \cdot \exp[-0.008(V + 28)]}{1 + \exp[0.15(V + 28)]}$$

$$\beta_f = \frac{0.0065 \cdot \exp[-0.02(V + 30)]}{1 + \exp[-0.2(V + 30)]}$$

$$d([Ca]_i) / dt = -10^{-4} \cdot I_{Ca} + 0.07(10^{-4} - [Ca]_i)$$

$$dy/dt = (y_\infty - y)/\tau_y \quad y_\infty = \frac{\alpha_y}{\alpha_y + \beta_y} \quad \tau_y = \frac{1}{\alpha_y + \beta_y}$$

$$I_{k1} = \bar{G}_{k1} \cdot K1_\infty \cdot (V - E_{k1}),$$

$$\bar{G}_{k1} = 0.6047 \cdot \sqrt{[K]_0} / 5.4$$

$$\alpha_{K1} = \frac{1.02}{1 + \exp[0.2385 \cdot (V - E_{K1} - 59.215)]}$$

$$\beta_{k1} = \frac{0.49124 \cdot \exp[0.08032 \cdot (V - E_{k1} + 5.476)] + \exp[0.06175 \cdot (V - E_{k1} - 594.31)]}{1 + \exp[-0.5143 \cdot (V - E_{k1} + 4.753)]}$$

$$I_{Kp} = 0.0183 \cdot K_p \cdot (V - E_{Kp}),$$

$$E_{Kp} = E_{K1}$$

$$K_p = 1 / \{1 + \exp[(7.488 - V) / 5.98]\}$$

$$I_k = \bar{G}_k \cdot X \cdot X_i \cdot (V - E_k),$$

$$\bar{G}_k = 0.282 \cdot \sqrt{[K]_0} / 5.4.$$

For $V > -100mV$

$$X_i = \frac{2.837 \cdot \{\exp[0.04(V + 77)] - 1\}}{(V + 77) \cdot \exp(0.04(V + 35))}$$

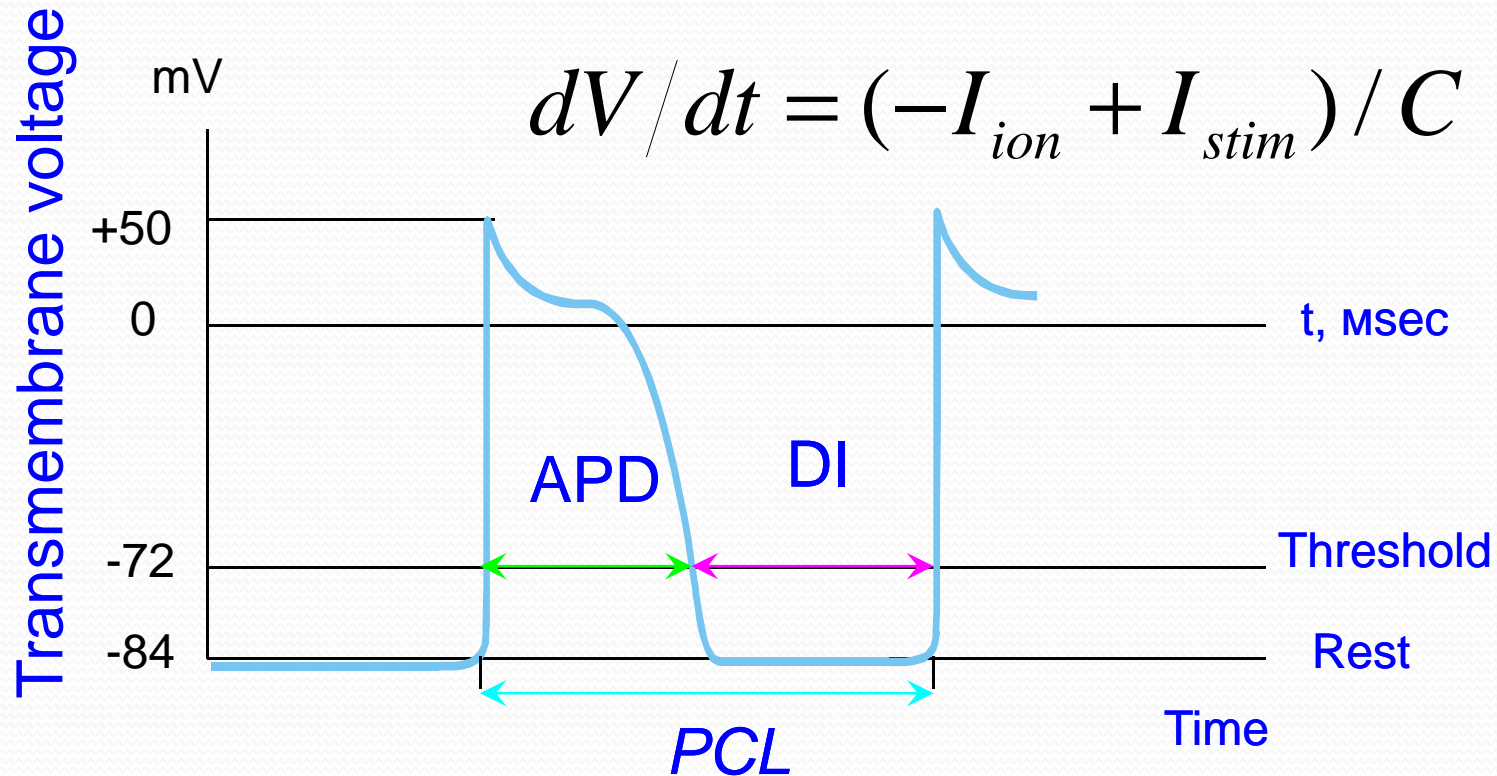
$X_i = 1$ for $V \leq -100mV$

$$\alpha_x = \frac{0.0005 \cdot \exp[0.083(V + 50)]}{1 + \exp[0.057(V + 50)]}$$

$$\beta_x = \frac{0.0013 \cdot \exp[-0.06(V + 20)]}{1 + \exp[-0.04(V + 20)]}$$

Luo-Rudy model

ACTION POTENTIAL

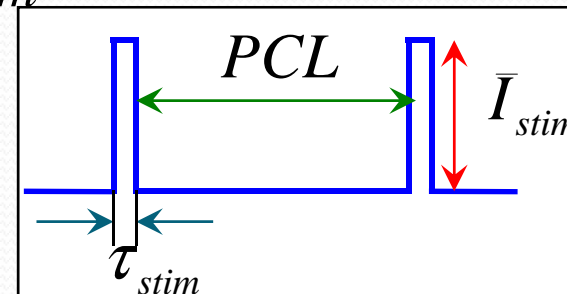


APD - action potential duration

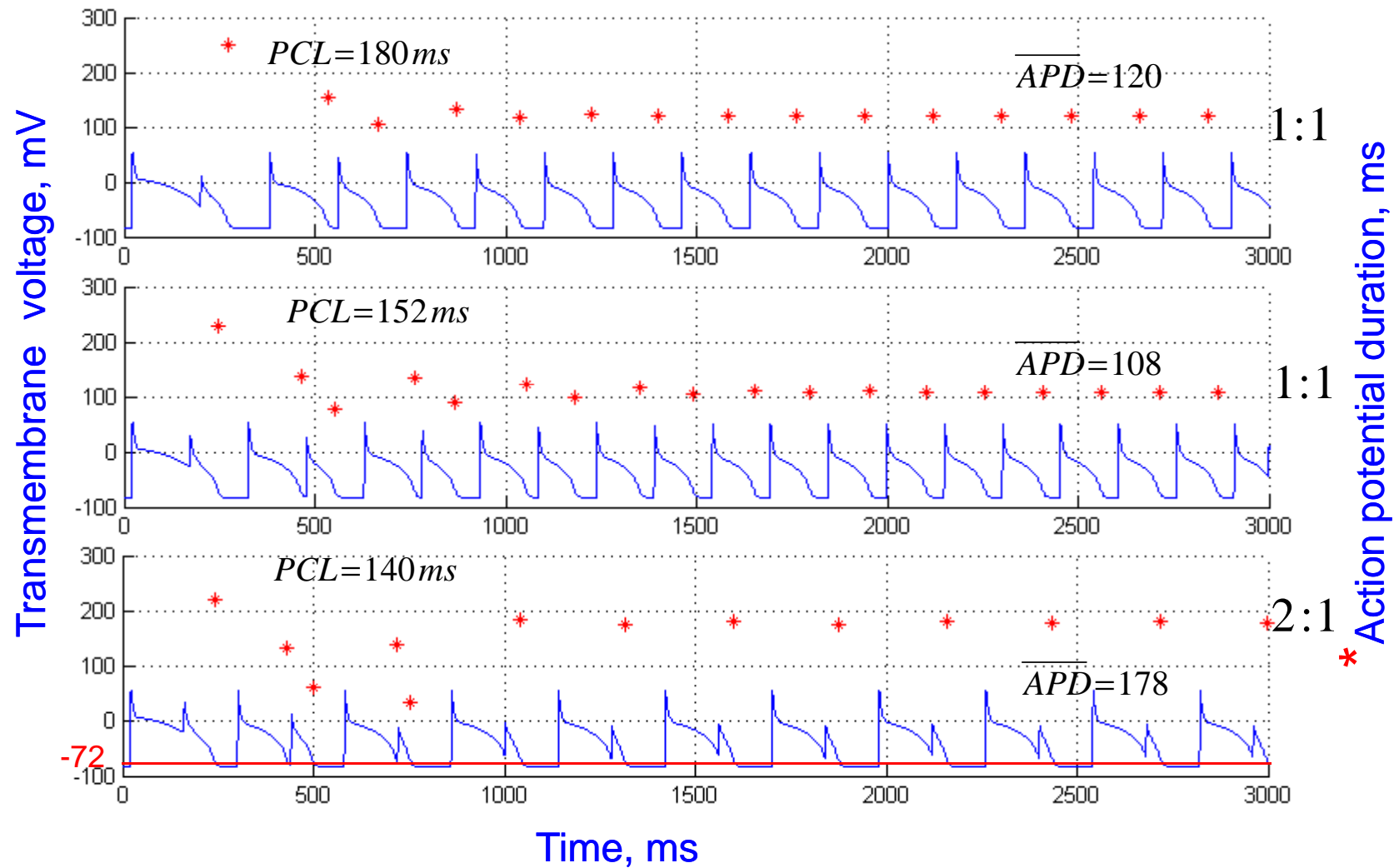
DI - diastolic interval

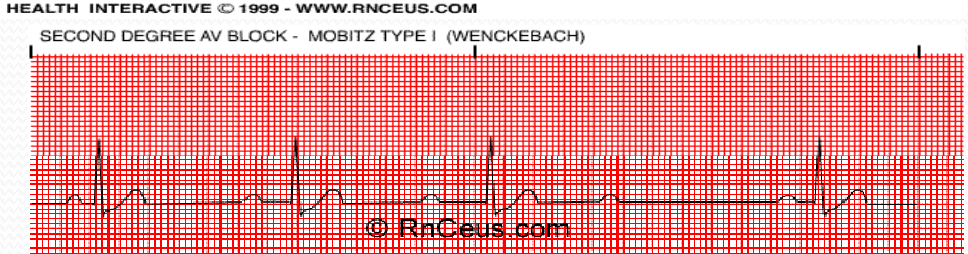
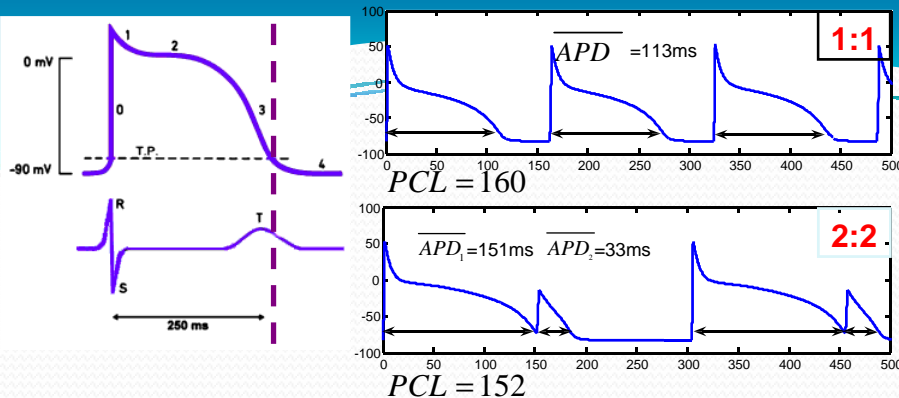
PCL - pacing cycle length

I_{stim} - stimulus current

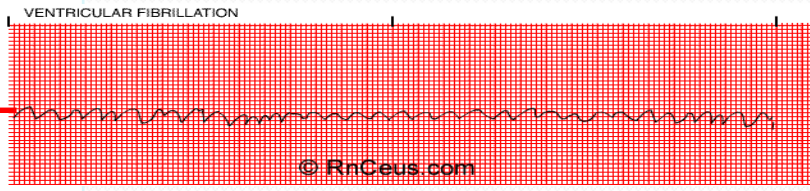
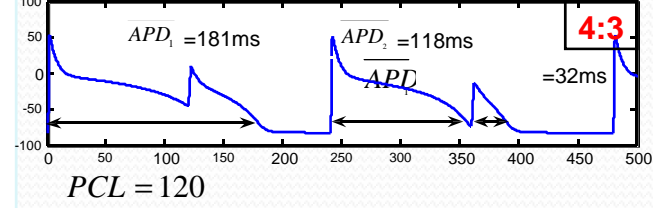
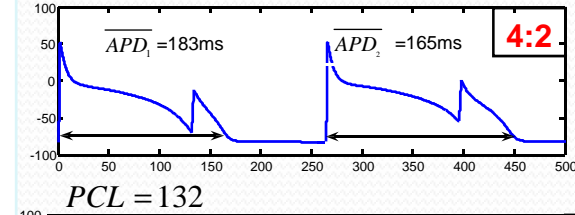
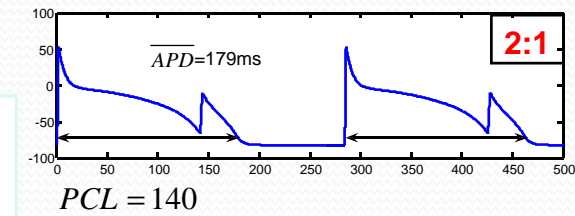
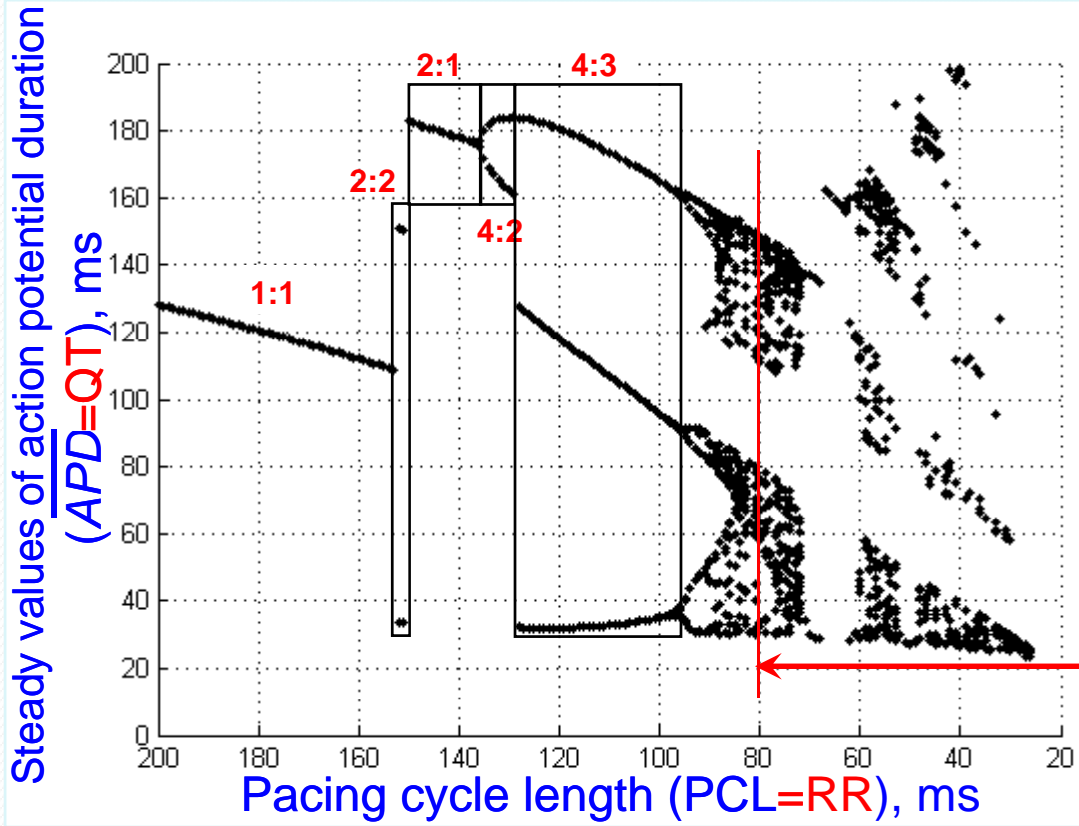


Steady states of action potential duration





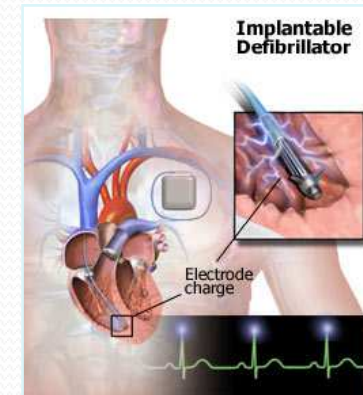
Bifurcation diagram



$$I_{st} = 30 \mu A / cm^2$$

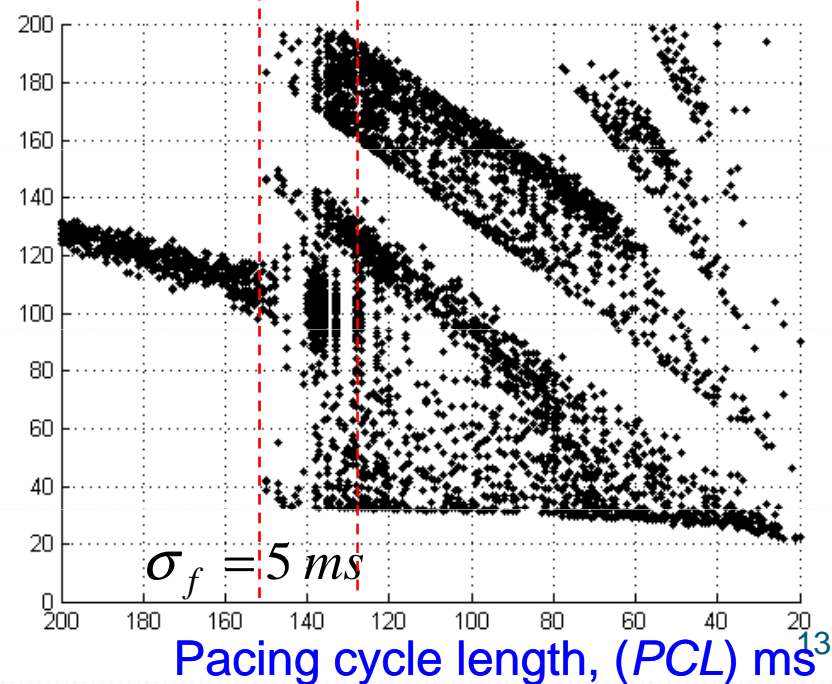
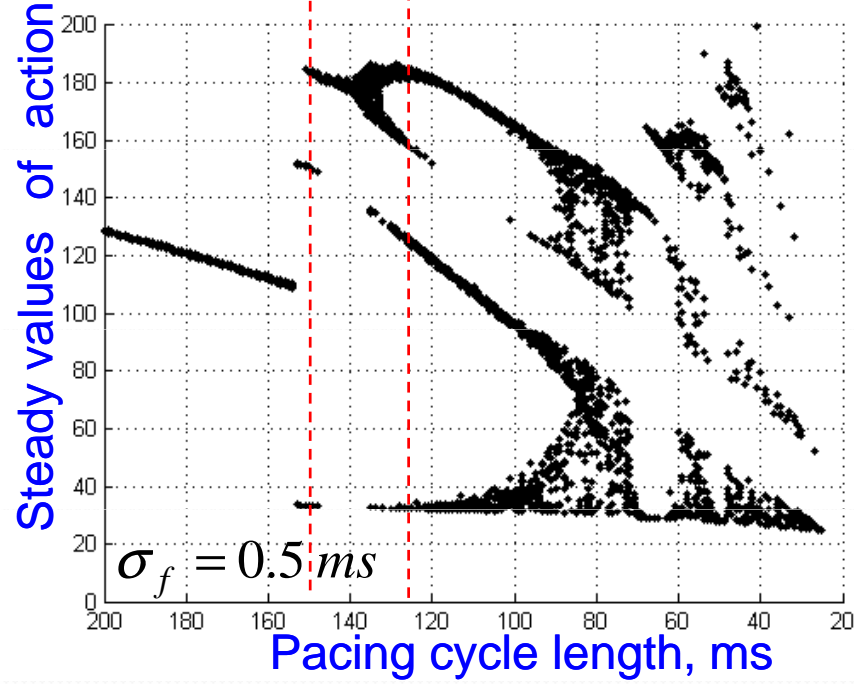
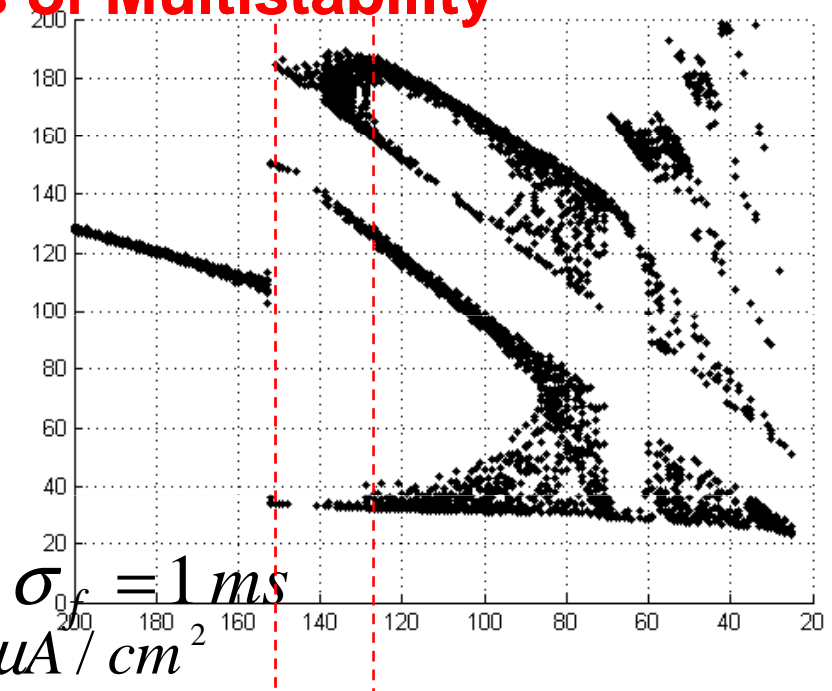
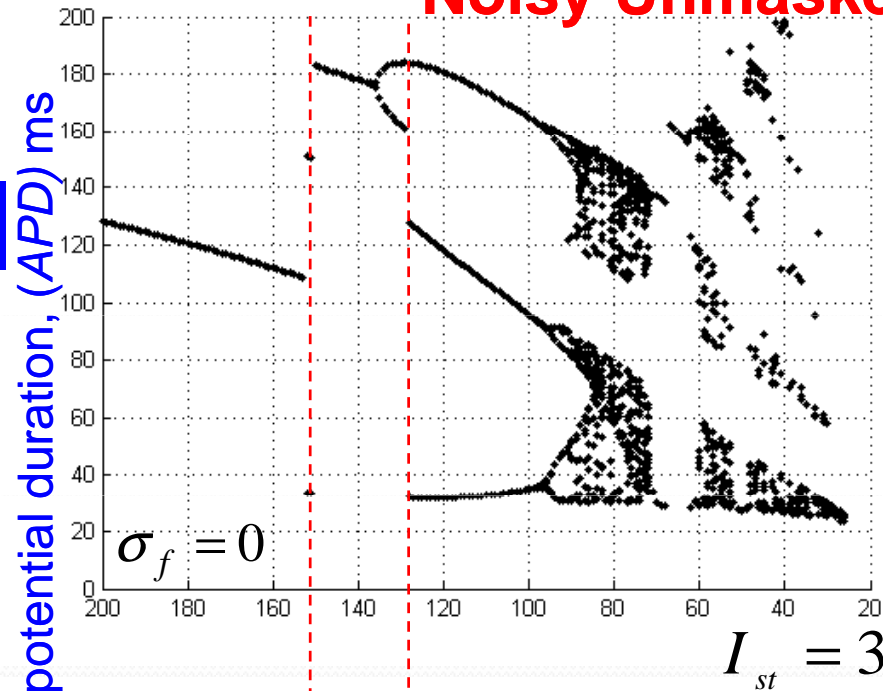
Michael Rubart and Douglas P. Zipes, Mechanisms of sudden cardiac death, *J. Clin. Invest.* 115,2305 (2005).

“While the implantable cardioverter defibrillator (ICD) improves survival in high-risk patients , standard antiarrhythmic drug therapy has failed to reduce, and in some instances has increased, the incidence of SCD.



In fact, the greatest reduction in cardiovascular mortality (including SCD) in patients with clinically manifest heart disease has resulted from the use of beta blockers and non-antiarrhythmic drugs”

Noisy Unmaskers of Multistability



Experimental observations of bi-stability in cardio dynamics



- G. R. Mines, “On dynamic equilibrium in the heart,” J. Physiol. London 46, 349–383 ,1913.
- Yehia, A.R., Jeandupeux, D., Alonso, F., Guevara, M.R., Hysteresis and bi-stability in the direct transition from 1:1 to 2:1 rhythm in periodically driven single ventricular cells. Chaos 9 (4) (1999), 916–931.
- Guevara M.R., Ward G., Shrier A., Glass L., Electrical alternans and period-doubling bifurcations. In: Computers in Cardiology. IEEE Computer Society, Silver Spring, MD, (1984) 167–170.
- Goldhaber, J. I., Xie, L. H., Duong, T, Motter, C., Khuu, K, and Weiss, J. N. (2005). Action potential duration restitution and alternans in rabbit ventricular myocytes: the key role of intracellular calcium cycling, Circ. Res. 96, pp. 459–466.

Hysteresis and bistability in the direct transition from 1:1 to 2:1 rhythm in periodically driven single ventricular cells

Ali R. Yehia, Dominique Jeandupeux, Francisco Alonso, and Michael R. Guevara^{a)}
*Department of Physiology and Centre for Nonlinear Dynamics in Physiology and Medicine,
 McGill University, Montréal, Québec H3G 1Y6, Canada*

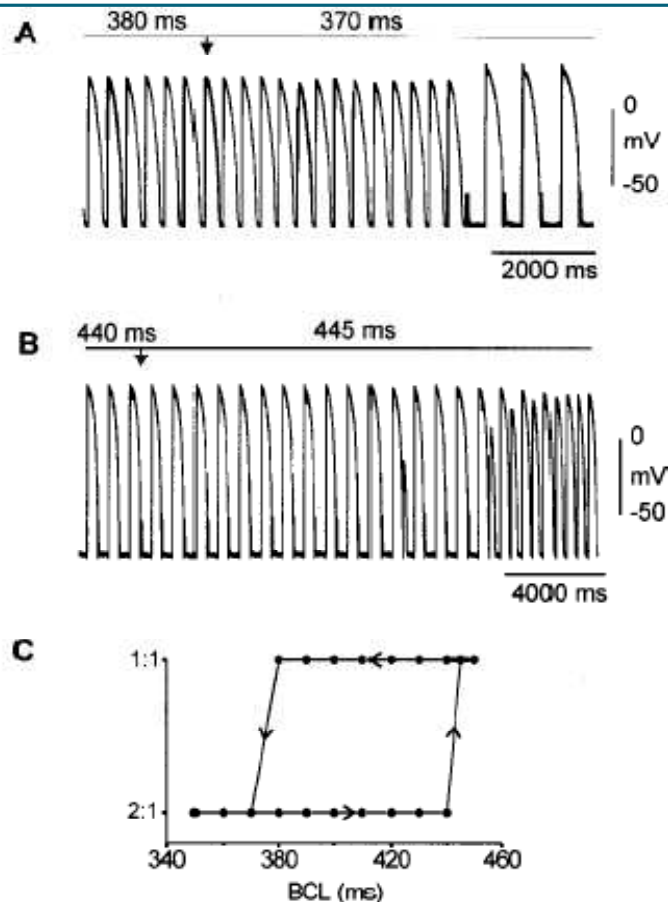


FIG. 1. Hysteresis in $\{1:1\} \leftrightarrow \{2:1\}$ transition (experiment). (A) $\{1:1\} \rightarrow \{2:1\}$ transition. Transmembrane potential plotted vs time. Arrow indicates beginning of first cycle with BCL=370 ms. (B) $\{2:1\} \rightarrow \{1:1\}$ transition. Arrow indicates beginning of first cycle with BCL=445 ms. (C) Hysteresis loop. Stimulus artefacts due to imperfect bridge balance retouched in (A) and (B) and all subsequent experimental traces by erasing part of the deflection; thus voltage during time of stimulus pulse injection is only an estimate made based on recordings from other cells with negligible stimulus artefact. Pulse amplitude=850 pA, pulse duration=5 ms.

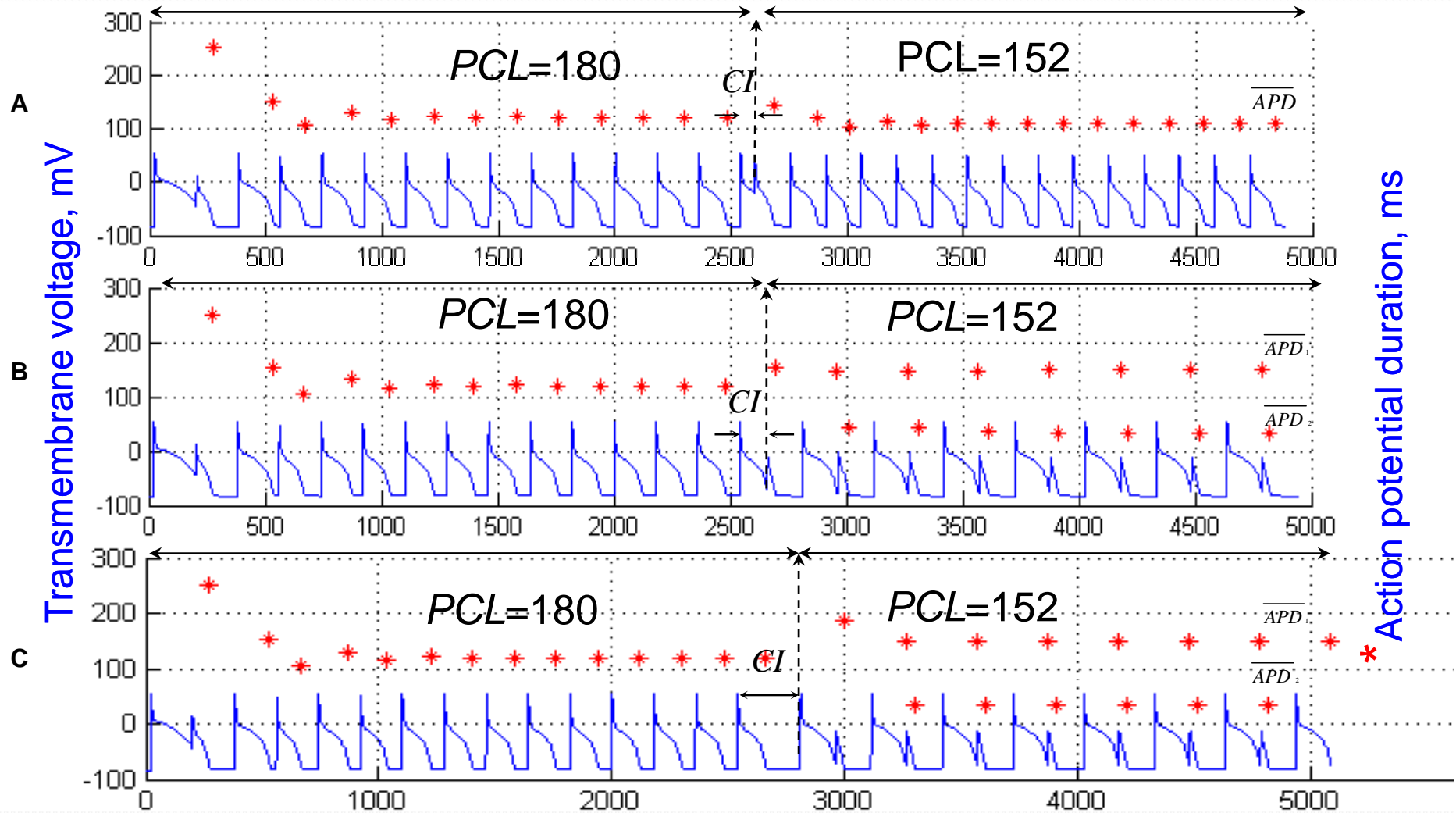
The average stimulus amplitude at which the direct $\{1:1\} \rightarrow \{2:1\}$ transition was seen was ~ 1.2 times the threshold amplitude needed to obtain 1:1 rhythm at BCL=1000 ($n=12$). In all cells in which the direct $\{1:1\} \rightarrow \{2:1\}$ transit was found, and in which an alternans or Wenckebach rhythm (e.g., 3:2 rhythm) was also encountered at a different pulse amplitude, alternans occurred at a pulse amplitude higher than that at which the $\{1:1\} \rightarrow \{2:1\}$ transition occurred (e.g., alternans was seen in the cell of Fig. 1 at an amplitude of 900 pA), while Wenckebach rhythm occurred at a lower pulse amplitude.

B. Hysteresis between 1:1 and 2:1 rhythms

Following the direct transition from 1:1 to 2:1 rhythm, further decrease in BCL resulted in 2:1 rhythm being maintained over a range of BCL. The BCL was then gradually increased. In the experiment of Fig. 1, upon increasing BCL from 440 to 445 ms, the cell converted back from 2:1 to 1:1 rhythm [Fig. 1(B)]. Again, a transient was seen after the BCL was changed (arrow), this time consisting of several 2:1 cycles followed by several alternans cycles. As with the $\{1:1\} \rightarrow \{2:1\}$ transition, the transient was not the same from cell to cell or even from trial to trial, with the number of transient 2:1 cycles being between ~ 2 and ~ 15 . The fact that the $\{2:1\} \rightarrow \{1:1\}$ transition occurred at a longer BCL from that at which the $\{1:1\} \rightarrow \{2:1\}$ transition had initially occurred demonstrates the existence of hysteresis. We shall refer to this hysteresis between 1:1 and 2:1 rhythms as " $\{1:1\} \leftrightarrow \{2:1\}$ hysteresis." Figure 1(C) shows the hysteresis loop, which was ~ 75 ms wide in this cell. In each of five other cells in which the direct $\{1:1\} \rightarrow \{2:1\}$ transition was seen and in which a search for hysteresis was made, hysteresis was observed (hysteresis range=25–100 ms, $n=6$).

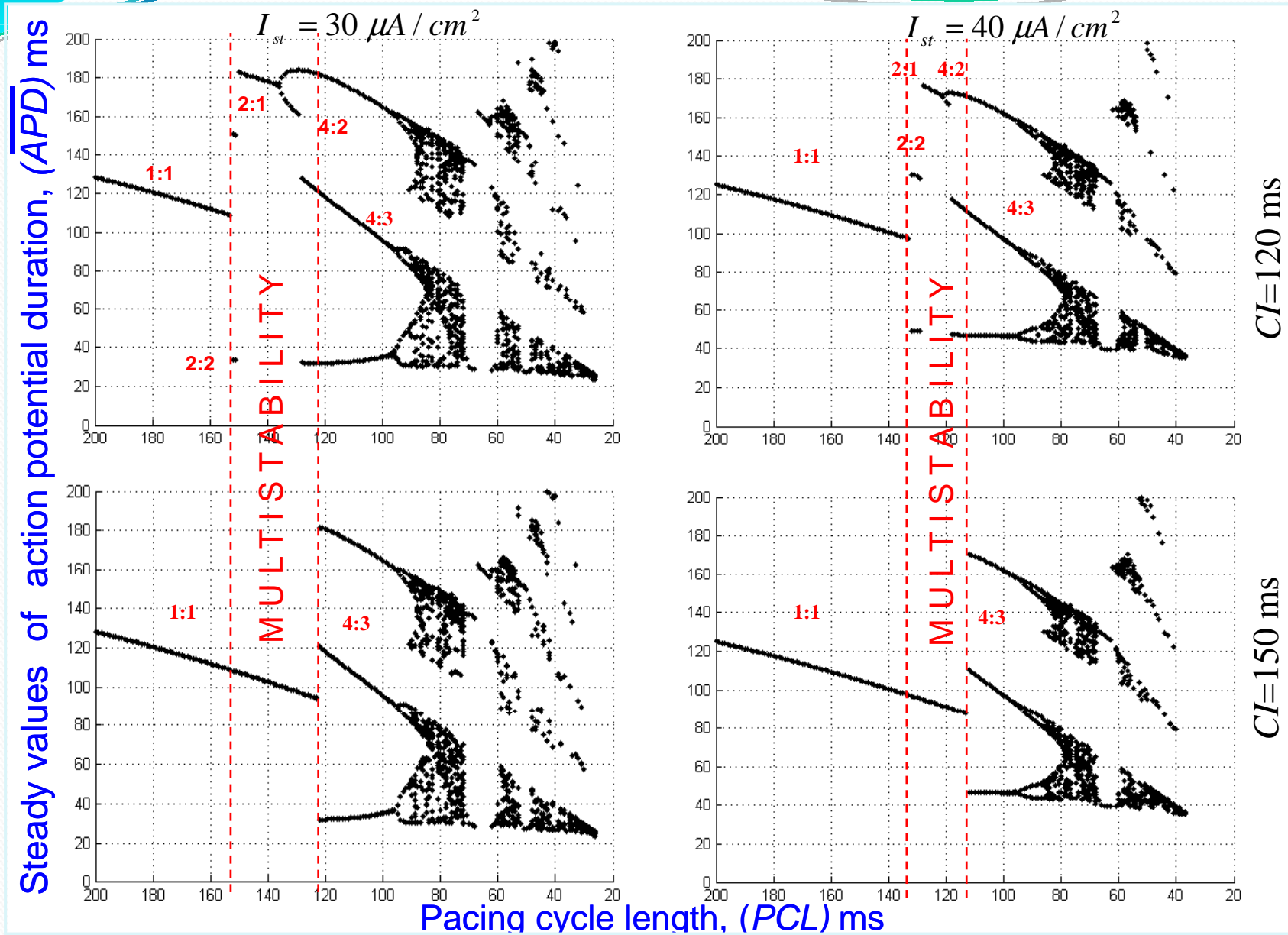
One possible explanation for hysteresis is that the elec-

Double-stage protocol of stimulation

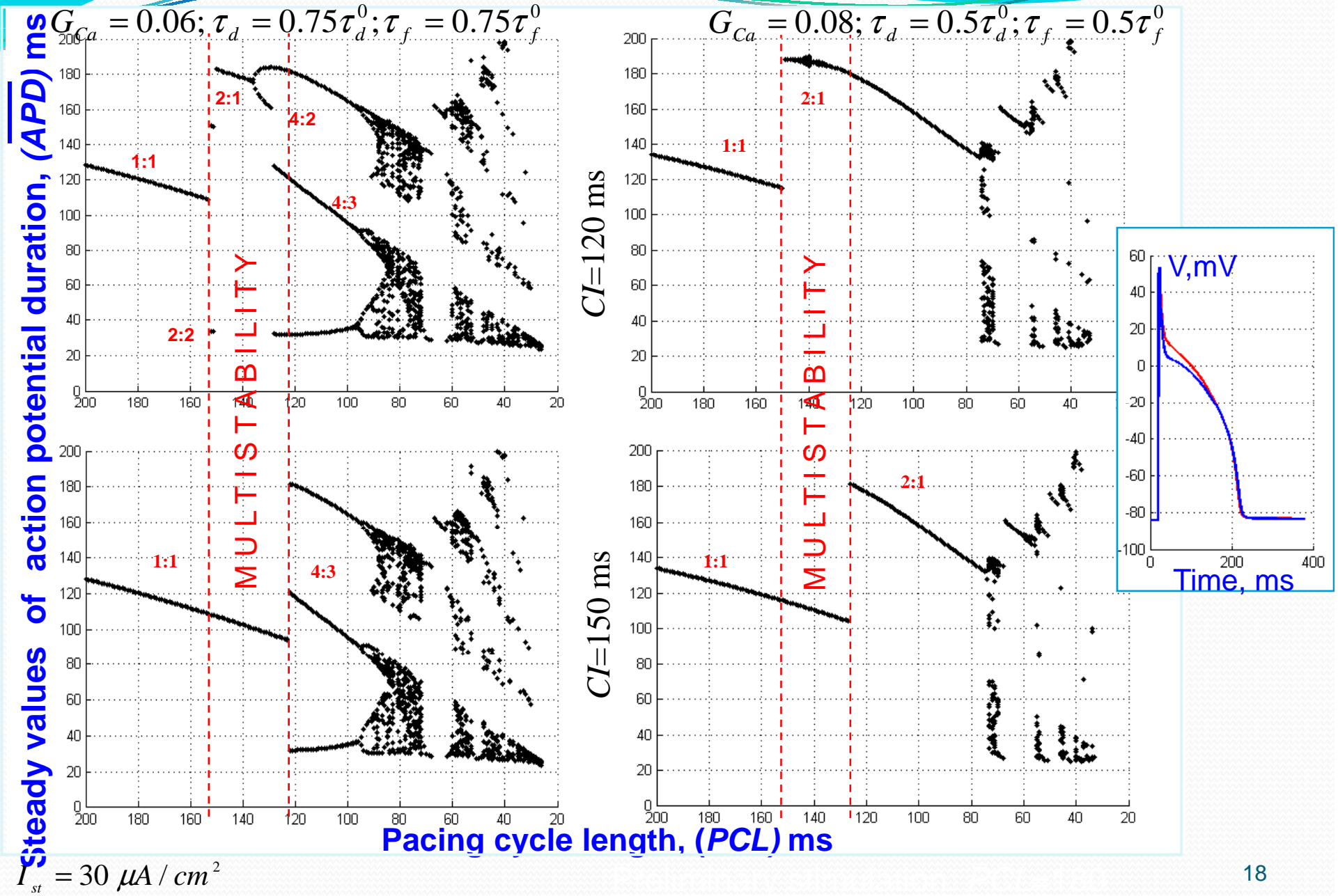


Multistability - the coexistence of different dynamical regimes of cardiac cell-model at a fixed set of stimulation parameters

Multistability as lability invariant

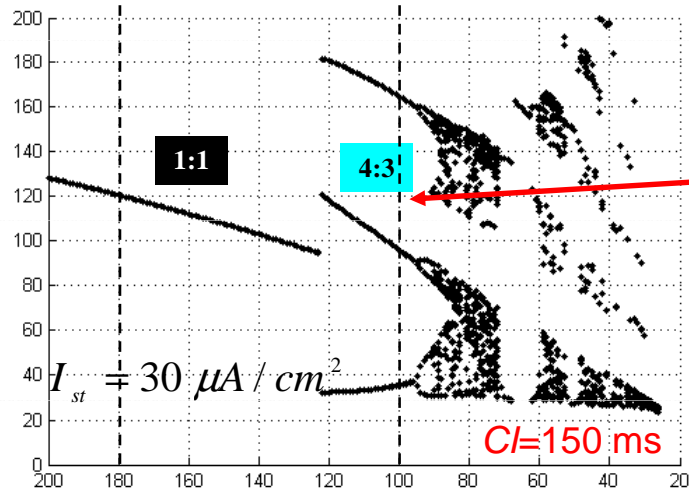
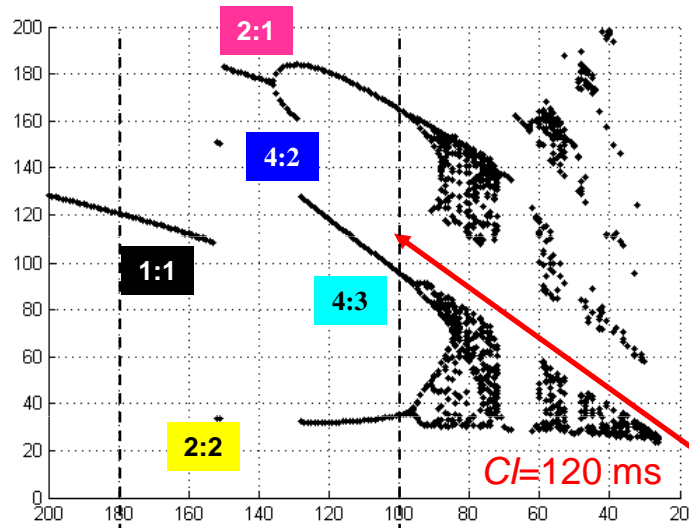


Multistability as variability invariant

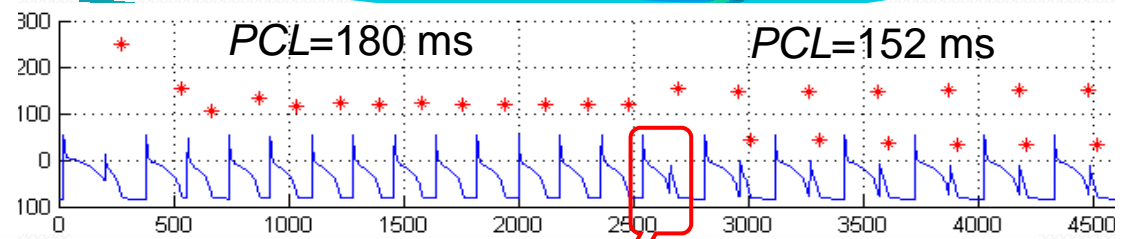


Basins of attraction - Vulnerable windows

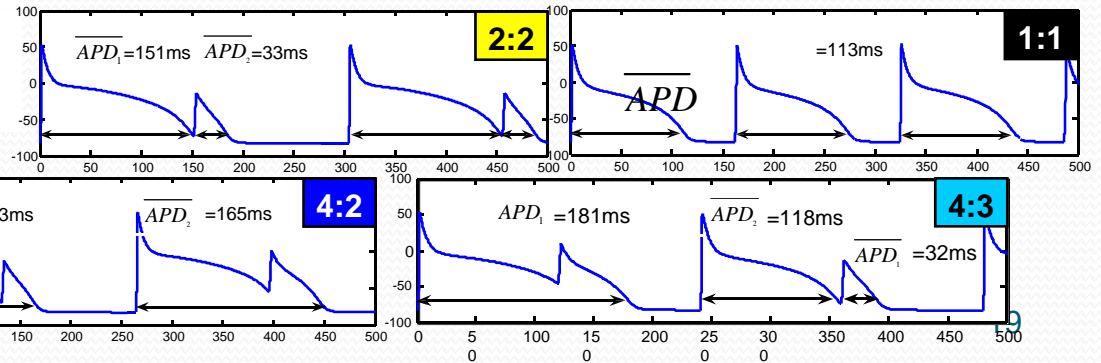
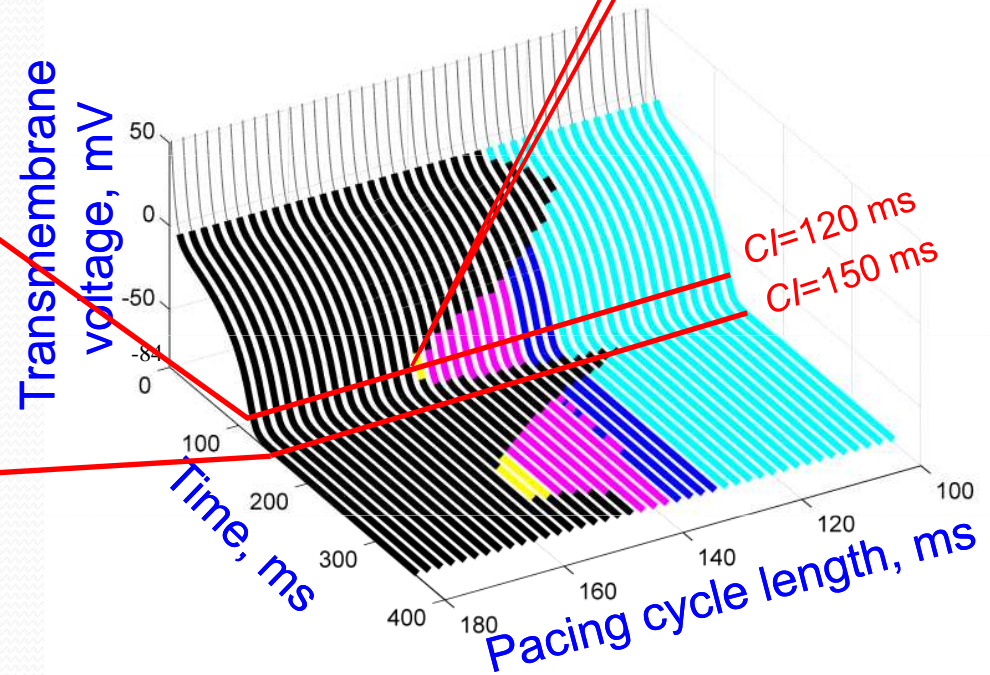
Steady values of action potential duration, ms



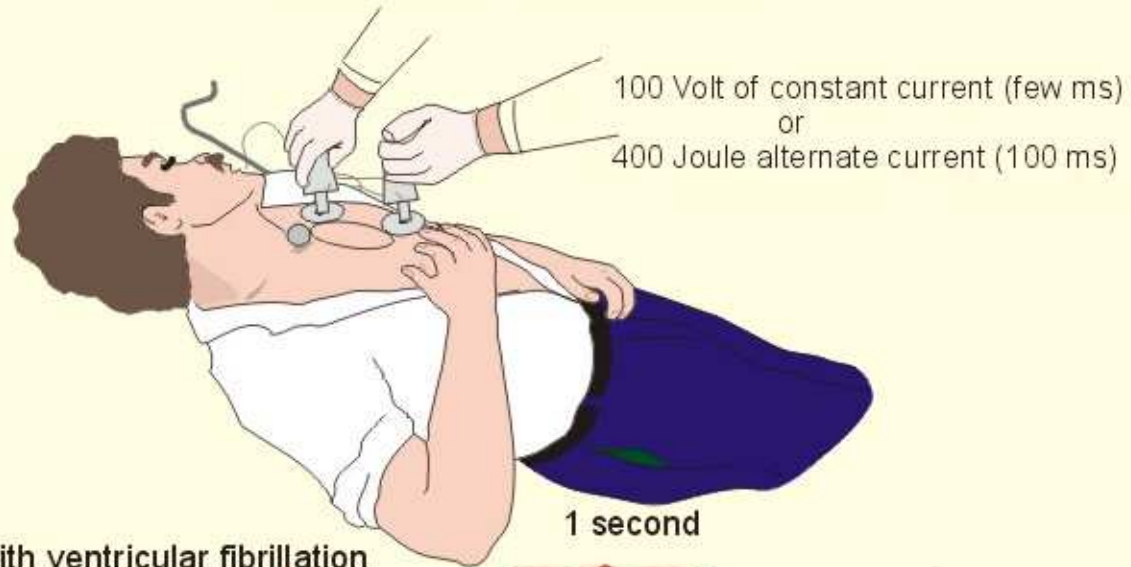
Pacing cycle length, ms



Transmembrane voltage, mV



Ventricular Defibrillation



ECG with ventricular fibrillation

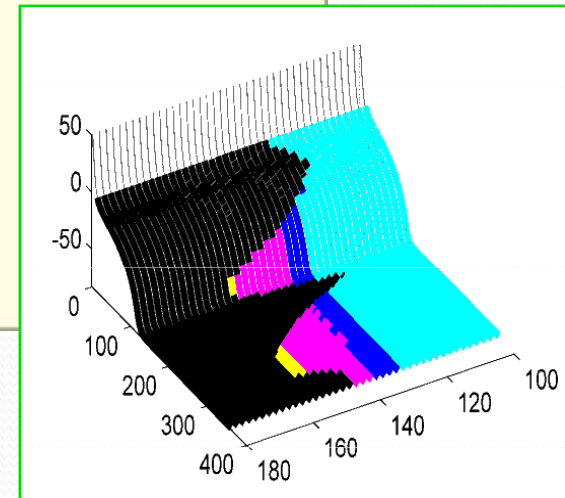


Ventricular action potential



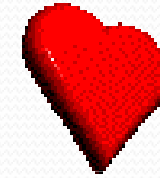
Vulnerable period (phase 3)

Fig. 11-10



Заключение

- Показана возможность использования бифуркационного анализа для поиска инвариантов в сложных системах.
- Установлен механизм мультистабильности в модели электрической проводимости клетки миокарда.
- Обнаружены бассейны притяжения устойчивых режимов на кривых потенциала действия миоцита, которые объясняют существование опасных окон уязвимости на ЭКГ-сигнале .
- Показано, что механизм мультистабильности инвариантен как по отношению к процессу управления, так и по отношению к вариабельности состояний клетки.



Stay in good health!
Listen to your heart....

Thank you!